Electronic Supplementary Material (ESI) for Sustainable Energy & Fuels.

Supporting information

Candle soot nanoparticles decorated wood for efficient solar vapor generation

Zhe Wang, Yutao Yan, Xiaoping Shen, Qingfeng Sun* and Chunde Jin*

School of Engineering, Zhejiang A & F University, Hangzhou 311300, China

***Corresponding author E-mail**: qfsun@zafu.edu.cn (Qingfeng Sun); jincd@zafu.edu.cn (Chunde Jin)

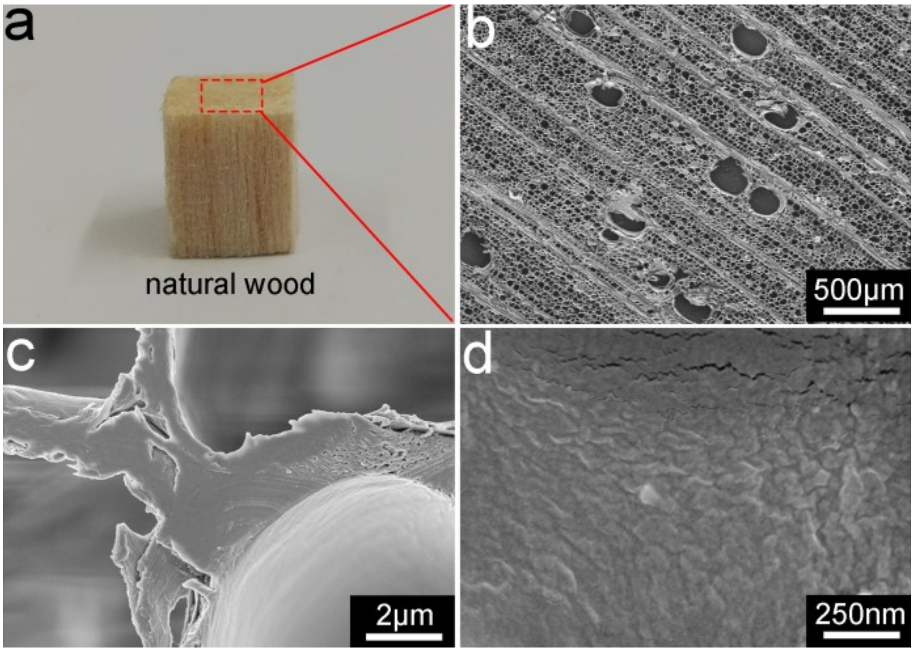

Fig. S1 (a) Photo image of natural wood. (b-d) Cross section SEM images of natural wood under different amplification.

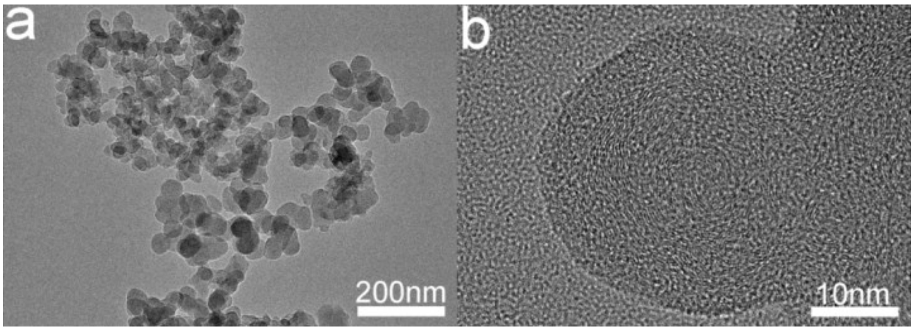

Fig. S2 TEM images of candle soot under different amplification.

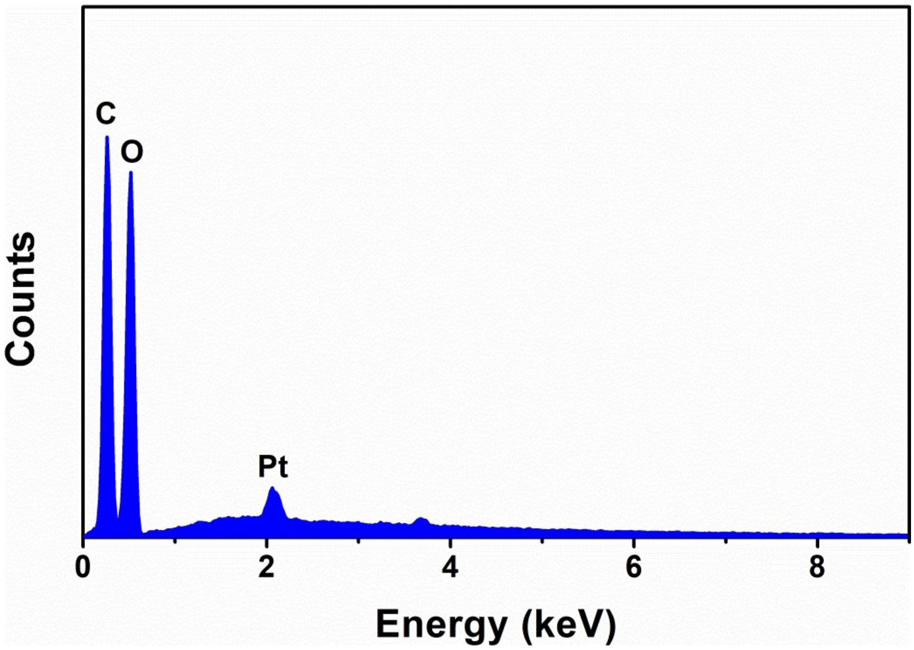

Fig. S3 Cross-section EDS of the pristine wood.

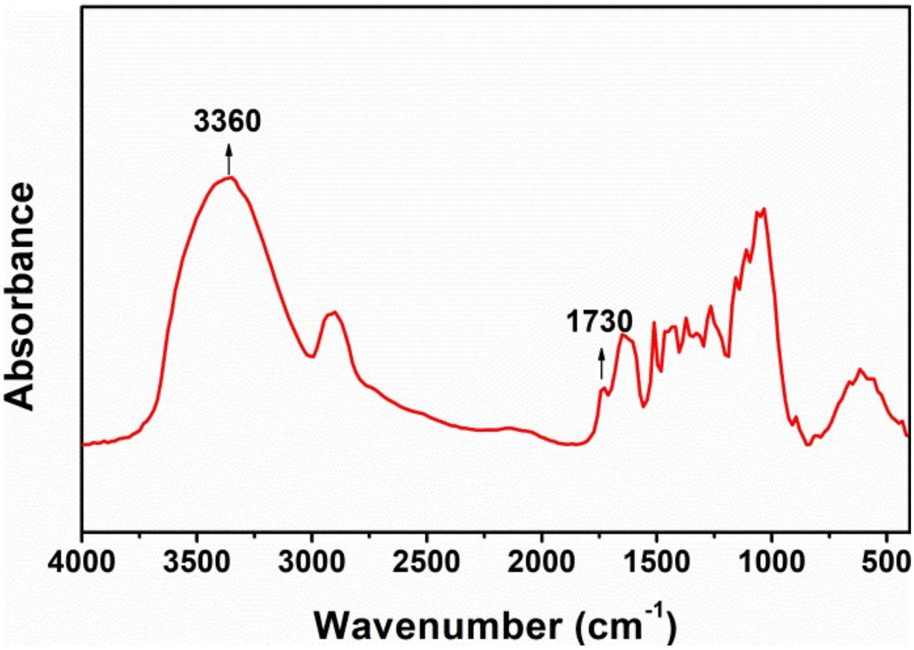

Fig. S4 FTIR of the wood substrate.

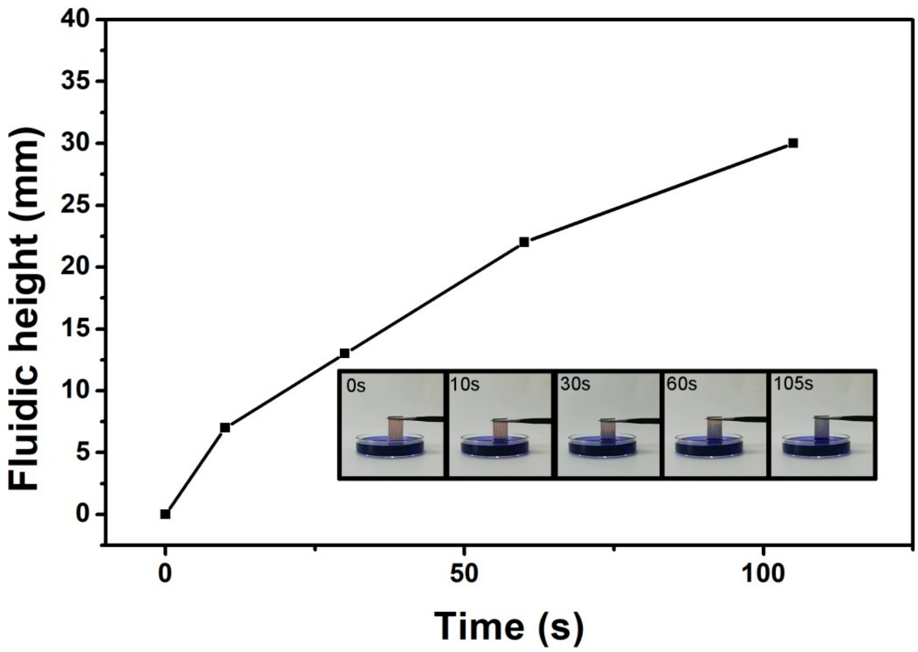

Fig. S5 The transportation of the methyl-blue aqueous solution along wood.

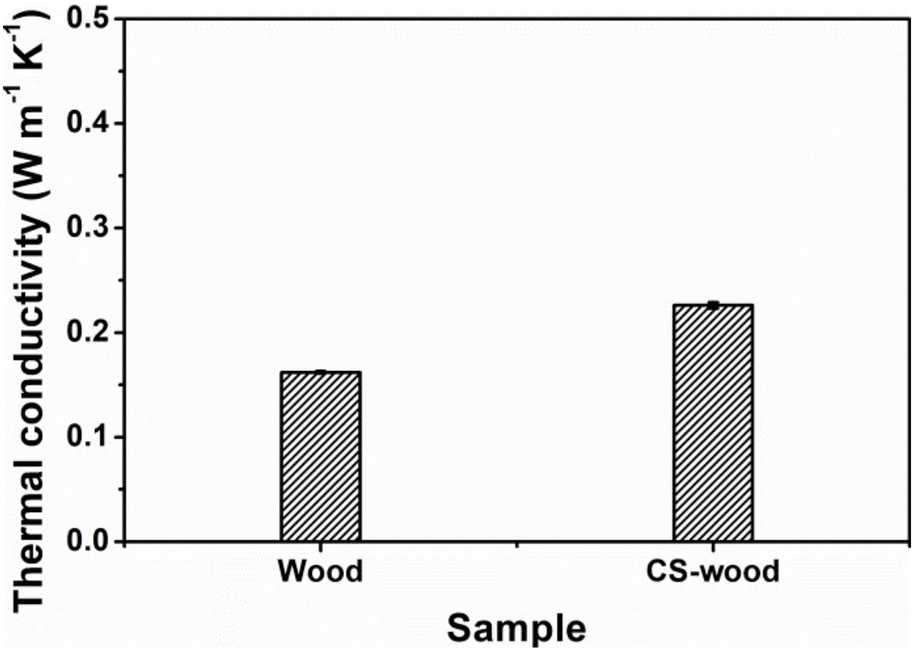

Fig. S6 Thermal conductivities of the pristine wood and CS-wood.

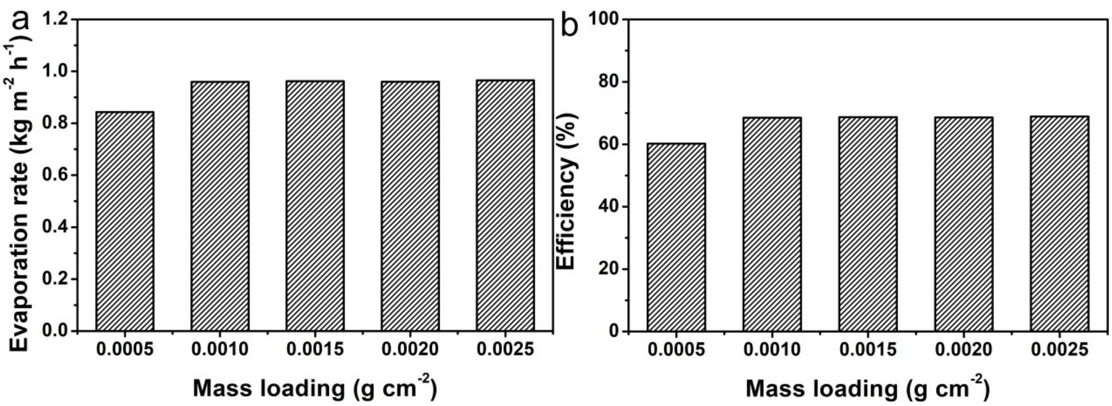

Fig. S7 Evaporation rate and efficiency of CS-wood device with different mass loadings of candle soot nanoparticles.

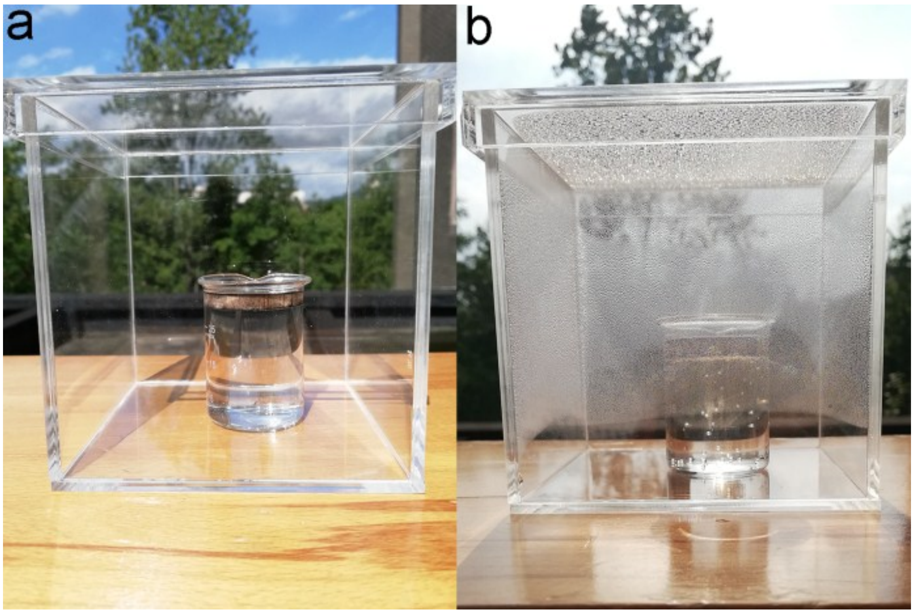

Fig. S8 Outdoor solar seawater desalination by CS-wood device under natural sunlight.

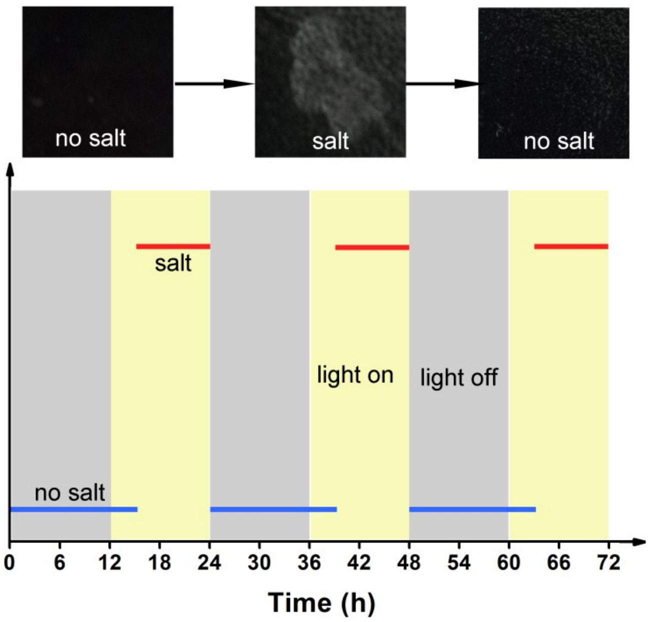

Fig. S9 The salt generates under illumination and dissolves automatically under dark conditions.

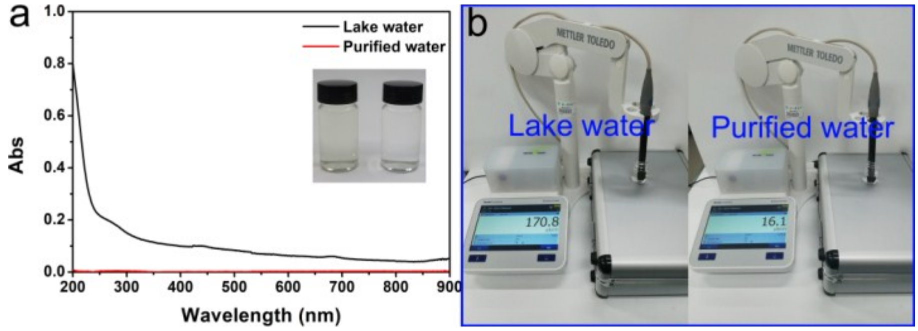

Fig. S10 (a) The absorption spectra of lake water and purified water (Insert: photo of lake water (left) and purified water (right). (b) Conductivity photograph of lake water and purified water.

Table S1. Solar vapor generation performances of CS-wood compared with other materials.

Sample	Power density (kW m^{-2})	Efficiency (%)	Ref
Functionalized graphene	1	48	1
Magnetic Fe_3O_4 decorated rGO	1	70	2
Carbon black	10	69±4	3
Graphene aerogel	1	53.6±2.5	4
rGO/PEI/mixed cellulose esters	1	60	5
Exfoliated graphite coated carbon foam	1	64	6
CNT decorated flexible wood	1	65	7
Bilayer wood with carbonized surface	1	57.3	8
PPy coated stainless steel mesh	1	≈58	9
Carbon black/PMMA/PAN	1	51	10
Plasmonic wood	1	≈67	11
Au/NPT	1	≈64	12
rGO/PU nanocomposite foam	1	65	13
Dopamine covered PU sponges	1	52.2	14
CS-wood	**1**	**68.5**	**This work**

Table S2. The main cationic concentrations (mg L^{-1}) of the seawater and desalted water.

Ions	Na^+	Mg^{2+}	K^+	Ca^{2+}
Seawater	10562.85	1086.32	492.46	417.40
Desalted water	2.08	0.54	0.86	1.26

Section 1. Bulk densities and porosities

The bulk densities and porosities measurements have been carried out on raw wood and CS-wood (mass loading of 0.001g cm^{-2}). The bulk densities of raw and CS-wood were calculated using the following formula:

$$\rho = \frac{m}{V} \quad (1)$$

where m and V are the weight and volume of the raw wood and CS-wood, respectively.

The bulk densities of the raw wood and CS-wood were 0.105g cm^{-3} and 0.106g cm^{-3} according to the above formula.

The porosity was calculated using the following equation:

$$porosity\ (\%) = \left(1 - \frac{\rho}{\rho_s}\right) \times 100 \quad (2)$$

where ρ and ρ_s are the volumetric mass densities of the wood (or CS-wood) and corresponding solid scaffold (wood cell wall and CS treated wood cell wall) , respectively.

Considering that the CS treated material can be regarded as a composite of wood and CS, its density was calculated according to the following equation:

$$\rho_s = \frac{1}{\frac{\omega_{wood}}{\rho_{wood}} + \frac{\omega_{CS}}{\rho_{CS}}} = \frac{1}{\frac{1 - \omega_{CS}}{\rho_{wood}} + \frac{\omega_{CS}}{\rho_{CS}}} \quad (3)$$

where ω_{wood} is the weight fraction of wood in the CS-wood and ω_{CS} is the weight fraction of CS. ρ_{wood} was fixed at 1.5 g cm^{-3} based on literature data[15,16] and ρ_{CS} at 0.081 g cm^{-3} according to the data measured in this study. ω_{CS} was estimated as follows:

$$\omega_{CS} = \frac{m_{CS-wood} - m_{wood}}{m_{CS-wood}} \times 100 \quad (4)$$

where $m_{\mathrm{CS\text{-}wood}}$ and m_{wood} are the dry weights of the CS-wood and raw wood, respectively.

According to formula (2) and (3), the raw wood porosity was calculated: (1-0.105/1.5)×100, the obtained result was 93.0%.

According to formula (2), (3) and (4), the PPy-wood porosity was calculated: $(1-0.106/1.28)\times100$, the obtained result was 91.7%.

Section 2. Energy loss of solar vapor generation system.

The energy loss of the evaporation system mainly involves radiation loss, convection loss and conduction loss. The energy loss of the solar evaporation system under illumination is composed of 1) radiation loss P_{rad}, 2) convection loss P_{conv} and 3) conduction loss P_{cond}, detailed energy loss analysis was performed as following calculations.

Radiation:

The radiation flux P_{rad} can be calculated by Stefan-Boltzmann law.

$$P_{rad}=\varepsilon A\sigma(T_1^4-T_2^4) \quad (1)$$

Where P_{rad} denotes radiation heat flux, ε is the emissive rate (It is assumed that the absorber has a maximum emissivity of 1.00), A is the surface area, σ is the Stefan-Boltzmann constant (assumed to be 5.67×10^{-8} W m^{-2} K^{-4}), T_1 is the average temperature of the absorber (~34.7°C), and T_2 is the ambient temperature (~28°C). As a result, the radiation heat flux is estimated to be 43 W/m^2, and the radiation loss rate is about 4.3%.

Convection:

The convection loss P_{conv} can be calculated by Newton's law of cooling.

$$P_{conv}=h(T_1-T_2) \quad (2)$$

where P_{conv} denotes convection heat flux, h is the convection heat transfer coefficient (assumed to be 10 W m^{-2} K^{-1}). Here, the convection heat is estimated as ≈ 67 W/m^2, and the convection loss rate is about 6.7%.

Conduction:

Conduction loss P_{cond} is based on Fourier's law.

$$P_{cond}=Cm\Delta T \quad (3)$$

Where C is the specific heat capacity of water (4.2 J °C^{-1} g^{-1}), m denotes the weight of bulk water and ΔT represents the increased temperature of the bulk water after stable steam generation. In this work, m = 10 g, ΔT = 2.0 °C. Thus, the conductive loss is about 233 W m^{-2} and the conductive heat loss rate is about 23.3 %.

References

1. J. Yang, Y. Pang, W. Huang, S. K. Shaw, J. Schiffbauer, M. A. Pillers, X. Mu, S. Luo, T. Zhang, Y. Huang, G. Li, S. Ptasinska, M. Lieberman and T. Luo, *ACS*

Nano, 2017, **11**, 5510-5518.
2. X. Wang, G. Ou, N. Wang and H. Wu, *ACS Appl. Mater. Interfaces*, 2016, **8**, 9194-9199.
3. G. Ni, N. Miljkovic, H. Ghasemi, X. Huang, S. V. Boriskina, C.-T. Lin, J. Wang, Y. Xu, M. M. Rahman, T. Zhang and G. Chen, *Nano Energy*, 2015, **17**, 290-301.
4. Y. Fu, G. Wang, T. Mei, J. Li, J. Wang and X. Wang, *ACS Sustainable Chem. Eng.*, 2017, **5**, 4665-4671.
5. G. Wang, Y. Fu, X. Ma, W. Pi, D. Liu and X. Wang, *Carbon*, 2017, **114**, 117-124.
6. H. Ghasemi, G. Ni, A. M. Marconnet, J. Loomis, S. Yerci, N. Miljkovic and G. Chen, *Nat. commun.*, 2014, **5**, 4449.
7. C. Chen, Y. Li, J. Song, Z. Yang, Y. Kuang, E. Hitz, C. Jia, A. Gong, F. Jiang, J. Y. Zhu, B. Yang, J. Xie and L. Hu, *Adv. Mater.*, 2017, **29**, 1701756.
8. M. Zhu, Y. Li, G. Chen, F. Jiang, Z. Yang, X. Luo, Y. Wang, S. D. Lacey, J. Dai, C. Wang, C. Jia, J. Wan, Y. Yao, A. Gong, B. Yang, Z. Yu, S. Das and L. Hu, *Adv. Mater.*, 2017, **29**, 1704107.
9. L. Zhang, B. Tang, J. Wu, R. Li and P. Wang, *Adv. Mater.*, 2015, **27**, 4889-4894.
10. W. Xu, X. Hu, S. Zhuang, Y. Wang, X. Li, L. Zhou, S. Zhu and J. Zhu, *Adv. Energy Mater.s*, 2018, **8**, 1702884.
11. M. Zhu, Y. Li, F. Chen, X. Zhu, J. Dai, Y. Li, Z. Yang, X. Yan, J. Song, Y. Wang, E. Hitz, W. Luo, M. Lu, B. Yang and L. Hu, *Adv. Energy Mater.*, 2018, **8**, 1701028.
12. Z. Lin, Y. Tan, D. Ji, B. Zhu, Z. Pei, J. Xu, Q. Gan, Z. Yu and Z. Jia, *Sci. Adv.*, 2016, **2**, e1501227.
13. G. Wang, Y. Fu, A. Guo, T. Mei, J. Wang, J. Li and X. Wang, *Chem. Mater.*, 2017, **29**, 5629-5635.
14. S. Ma, C. P. Chiu, Y. Zhu, C. Y. Tang, H. Long, W. Qarony, X. Zhao, X. Zhang, W. H. Lo and Y. H. Tsang, *Appl. Energy*, 2017, **206**, 63-69.
15. H. Guan, Z. Cheng and X. Wang, *ACS Nano*, 2018, **12**, 10365-10373.
16. Z. Zhang, G. Sèbe, D. Rentsch, T. Zimmermann, P. Tingaut, *Chem. Mater.*, 2014, **26**, 2659-2668.